

Tensor Calculus in Digital Colorimetry

Y. Saukova, M. Hundzina

Belarusian National Technical University,
Nezavisimosty Ave., 65, Minsk 220013, Belarus

Received 10.05.2022

Accepted for publication 17.08.2022

Abstract

Any object can have many implementations in the form of digital images and any digital image can be processed many times increasing or decreasing accuracy and reliability. Digital colorimetry faces the need to work out issues of ensuring accuracy, metrological traceability and reliability. The purpose of this work was to generalize approaches to the description of multidimensional quantized spaces and show the possibilities of their adaptation to digital colorimetry. This approach will minimize the private and global risks in measurements.

For color identification digital colorimetry uses standard color models and spaces. Most of them are empirical and are improved during the transition from standard to real observation conditions taking into account the phenomena of vision and the age of observers. From the point of view of measurement, a digital image can be represented by a combinatorial model of an information and measurement channel with the appearance of the phenomenon of a color covariance hypercube requiring a significant amount of memory for data storage and processing. The transition from the covariance hypercube to high-dimensional matrices and tensors of the first, second and higher ranks provides the prospect of optimizing the color parameters of a digital image by the criterion of information entropy.

Tensor calculus provides opportunities for expanding the dynamic range in color measurements describing multidimensional vector fields and quantized spaces with indexing tensors and decomposing them into matrices of low orders.

The proposed complex approach based on tensor calculus. According to this approach the color space is a set of directed vector fields undergoing sampling, quantization and coding operations. Also it is a dynamic open system exchanging information with the environment at a given level and to identify color with specified levels of accuracy, reliability, uncertainty and entropy.

Keywords: colorimetry, image, tensor, uncertainty, entropy.

DOI: 10.21122/2220-9506-2022-13-3-216-227

Адрес для переписки:

Савкова Е.Н.
Белорусский национальный технический университет,
пр-т Независимости, 65, г. Минск 220013, Беларусь
e-mail: savkova@bntu.by

Address for correspondence:

Saukova Y.
Belarusian National Technical University,
Nezavisimosty Ave., 65, Minsk 220013, Belarus
e-mail: savkova@bntu.by

Для цитирования:

Y. Saukova, M. Hundzina.
Tensor Calculus in Digital Colorimetry.
Приборы и методы измерений.
2022. – Т. 13, № 3. – С. 216–227.
DOI: 10.21122/2220-9506-2022-13-3-216-227

For citation:

Y. Saukova, M. Hundzina.
Tensor Calculus in Digital Colorimetry.
Devices and Methods of Measurements.
2022, vol. 13, no. 3, pp. 216–227.
DOI: 10.21122/2220-9506-2022-13-3-216-227

Тензорное исчисление в цифровой колориметрии

Е.Н. Савкова, М.А. Гундина

Белорусский национальный технический университет,
пр-т Независимости, 65, г. Минск 220013, Беларусь

Поступила 10.05.2022

Принята к печати 17.08.2022

Поскольку любой объект может иметь множество реализаций в виде цифровых изображений, а любое цифровое изображение может быть множество раз подвергнуто обработке, повышающей или понижающей точность и достоверность, цифровая колориметрия сталкивается с необходимостью проработки вопросов обеспечения точности, метрологической прослеживаемости и достоверности. Цель данной работы – обобщить подходы к описанию многомерных квантованных пространств и показать возможности их адаптации к цифровой колориметрии, что позволит минимизировать частные и глобальные риски, возникающие в измерениях.

Для идентификации цвета цифровая колориметрия использует стандартные цветовые модели и пространства, большинство из которых являются эмпирическими и совершенствуются при переходе от стандартных к реальным условиям наблюдения с учётом феноменов зрения и возраста наблюдателей. Цифровое изображение с точки зрения измерения может быть представлено комбинаторной моделью информационно-измерительного канала с возникновением феномена цветового ковариационного гиперкуба, требующего значительного объёма памяти для хранения и обработки данных. Переход от ковариационного гиперкуба к матрицам высоких размерностей и тензорам первого, второго и более высоких рангов предоставляет перспективу оптимизации цветовых параметров цифрового изображения по критерию информационной энтропии.

Тензорное исчисление предоставляет возможности расширения динамического диапазона в измерениях цвета, описания многомерных векторных полей и квантованных пространств с индексацией тензоров и разложением их на матрицы низких порядков.

Предложенный комплексный подход, основанный на тензорном исчислении, позволяет рассматривать цветовое пространство как совокупность направленных векторных полей, подвергающихся операциям дискретизации, квантования и кодирования, как динамическую открытую систему, обменивающуюся информацией с окружающей средой с заданным уровнем, и идентифицировать цвет с заданными уровнями точности, достоверности, неопределённости и энтропии.

Ключевые слова: колориметрия, изображение, тензор, неопределённость, энтропия.

DOI: 10.21122/2220-9506-2022-13-3-216-227

Адрес для переписки:

Савкова Е.Н.
Белорусский национальный технический университет,
пр-т Независимости, 65, г. Минск 220013, Беларусь
e-mail: savkova@bntu.by

Address for correspondence:

Saukova Y.
Belarusian National Technical University,
Nezavisimosty Ave., 65, Minsk 220013, Belarus
e-mail: savkova@bntu.by

Для цитирования:

Y. Saukova, M. Hundzina.
Tensor Calculus in Digital Colorimetry.
Приборы и методы измерений.
2022. – Т. 13, № 3. – С. 216–227.
DOI: 10.21122/2220-9506-2022-13-3-216-227

For citation:

Y. Saukova, M. Hundzina.
Tensor Calculus in Digital Colorimetry.
Devices and Methods of Measurements.
2022, vol. 13, no. 3, pp. 216–227.
DOI: 10.21122/2220-9506-2022-13-3-216-227

Introduction

Digital colorimetry focused on qualitative and quantitative methods for determining color from digital images faces the need to work out issues of ensuring accuracy, metrological traceability and reliability, since any object can have many implementations in the form of digital images, and any digital image can be processed many times, increasing or decreasing accuracy and reliability. It is because any object can have many implementations in the form of digital images, and any digital image can be processed many times, increasing or decreasing accuracy and reliability. Basic colorimetry assumes normalized observation conditions, and higher colorimetry includes “methods for assessing the perception of a color stimulus presented to an observer in a complex environment that we observe in everyday life” [1]. Methods of transmitting color information of an image in telecommunication systems are based on the use of the principles of higher colorimetry [2]. The concepts of “absolute” (differential) and “relative” colorimetry take into account the possibilities of color reproduction of technical means [3]. The idea of differential colorimetry consists in determining minor color differences on conditional virtual scales being developed for example in express methods of analytical measurements using a smartphone [4] terrain studies using satellite images [5, 6]. Relative colorimetry takes place in color-rendering systems allowing colors to be shifted taking into account the movement of the “white point” to a new position taking into account the limitations of the color coverage of technical devices [3, 7]. At the same time, there is a need to expand the dynamic range of digital images objectively limited by the color coverage of recording, transmitting and displaying devices in order to bring them as close as possible to the dynamic range of human vision ($0.000001\text{--}100000000\text{ cd/m}^2$) [8, 9].

In areas not related to measurements (television, computer games and design) multilayer HRDI images are used [8] to improve their visual perception with the transition from standard (SDR) $005\text{--}100\text{ cd/m}^2$ to high (HDR) $0.0005\text{--}10000\text{ cd/m}^2$ dynamic range and vice versa using special transfer functions in accordance with the recommendations of BT.709 [10], BT.1886 [11], BT.2100 [12] of the International Telecommunication Union (ITU). At the same time, traceability is ensured by setting “white”, “black”, 18 % and 75 % brightness levels

adaptable to a standard monitor and standard observation conditions [12]. The sources of metrological traceability of color in measurements are standards (standard samples, reference measuring instruments) and reference measurement techniques that serve to establish reference points of conditional virtual scales in color spaces. The issues that arise when expanding the dynamic range of digital images are as follows: 1) should the measurement results be viewed each time in a new interpretation of the color space, or should the same space be used? 2) is the color space static or a dynamic system? According to the authors, when implementing the measurement the color space should be considered as an open dynamic system taking into account the operations of sampling and quantization from the stand point of a single integrated approach based on tensor calculus. A large number of works are devoted to the development in colorimetry of the concept of a color tensor in relation, however, to the development of an equidistant color space [13]. We are interested in the further development of this topic namely the issues of dynamic range and quantization of spaces that have found application in theoretical physics.

The purpose of this work was to generalize approaches to the description of multidimensional quantized spaces and to show the possibilities of their adaptation to digital colorimetry, which will minimize private and global risks arising in measurements.

The problem of color multivariance and the phenomenon of covariance hypercube

A digital image is an information model “an image more or less similar (but not identical) to the depicted object” [14] described according to ISO/IEC 19794-5¹ by a two-dimensional representation of the brightness and texture of an object under certain lighting conditions, a discrete-continuous structure consisting of a finite number of elements (pixels) each of which has a geometric reference to the displayed object and its state in time. Color measurement consists in determining the color coordinates in the hardware-dependent *RGB* color space by averaging the intensity values in the red (*R*), green (*G*) and blue (*B*) color channels over the selected

¹ ISO/IEC 19794-5:2011 Information technology – Biometric data interchange formats. Part 5: Face image data

area of the digital image, comparing the obtained values with the built-in scale of virtual measures providing metrological traceability, transforming the obtained values into hardware-independent space (for example, XYZ) and the calculation of the chromaticity coordinates. Each control point on the surface of the object is an equally bright non-point emitter and the pixel area of the digital image corresponding to this control point is considered as a finite set of nominally identical intensity samples in the R, G, B color channels [15]. We understand by metrological traceability the property of the measurement result according to which the result can be correlated with the basis for comparison through a

documented unbroken chain of calibrations each of which contributes to the measurement uncertainty. The digital image is the result of convolution of the spectral distribution functions of the elements “illuminator”, “illuminated surface”, “recording device”, “software”, “display device” in the color space and an information model of any of them, provided that all other elements are validated [15].

If X_j is an input quantity (spectral distribution function or averaged intensity) the j -th element of the information and measurement channel and x_{kj} is the k -th random variable implementation with uncertainty $u(x_{ki}), I = 1, \dots, m$, then the parameter $u(x_{ki}, x_{lj})$ is the covariance of x_{ki} and x_{lj} as shown in Table.

Table

Validation model of the information and measurement channel

Realization K	Element j					Output param.
	Illuminator X_1	Illuminated surface X_2	Recording device X_3	Software X_4	Display device X_5	
K_1	x_{11} $u^2(x_{11})$	x_{12} $u(x_{12}, x_{21})$	x_{13} $u(x_{13}, x_{31})$	x_{14} $u(x_{14}, x_{41})$	x_{15} $u(x_{15}, x_{51})$	Y_1
K_2	x_{21} $u(x_{21}, x_{12})$	x_{22} $u^2(x_{22})$	x_{23} $u(x_{23}, x_{32})$	x_{24} $u(x_{24}, x_{42})$	x_{25} $u(x_{25}, x_{52})$	Y_2
K_3	x_{31} $u(x_{31}, x_{13})$	x_{32} $u(x_{32}, x_{23})$	x_{33} $u^2(x_{33})$	x_{34} $u(x_{34}, x_{43})$	x_{35} $u(x_{35}, x_{53})$	Y_3
K_4	x_{41} $u(x_{41}, x_{14})$	x_{42} $u(x_{42}, x_{24})$	x_{43} $u(x_{43}, x_{34})$	x_{44} $u^2(x_{44})$	x_{45} $u(x_{45}, x_{54})$	Y_4
K_5	x_{51} $u(x_{51}, x_{15})$	x_{52} $u(x_{52}, x_{25})$	x_{53} $u(x_{53}, x_{35})$	x_{54} $u(x_{54}, x_{45})$	x_{55} $u^2(x_{55})$	Y_5
...						
K_m	x_{m1} $u(x_{m1}, x_{1m})$	x_{m2} $u(x_{m2}, x_{2m})$	x_{m3} $u(x_{m3}, x_{3m})$	x_{m4} $u(x_{m4}, x_{4m})$	x_{m5} $u(x_{m5}, x_{5m})$	Y_m

The elements highlighted with a gray fill are measurement objects. Let's focus on implementations K_1-K_5 (implementations with two or more unknowns that increase information entropy are not considered here). The output parameter Y_k is defined by a set of chromaticity coordinates in a hardware independent space:

$$Y_k = A \begin{pmatrix} r \\ g \\ b \end{pmatrix}, \quad (1)$$

where A is the matrix of transition to the chromaticity coordinates of the hardware independent space; r, g, b are the chromaticity coordinates in space RGB [7]:

$$\begin{aligned}
 r &= \frac{R}{R+G+B}; \\
 g &= \frac{G}{R+G+B}; \\
 b &= \frac{B}{R+G+B},
 \end{aligned}
 \quad (2)$$

where R, G, B are color coordinates determined by averaging the intensities over a region of $M \times N$ pixels in the red, green and blue color channels of a digital image:

$$\begin{aligned}
 R &= \frac{1}{M N} \sum_{i=1}^M \sum_{k=1}^{N-1} R_{ik}; \\
 G &= \frac{1}{M N} \sum_{i=1}^M \sum_{k=1}^{N-1} G_{ik}; \\
 B &= \frac{1}{M N} \sum_{i=1}^M \sum_{k=1}^{N-1} B_{ik}.
 \end{aligned}
 \quad (3)$$

In turn, each element of the information-measuring channel, described by the value X_j , can be represented by a set of W variables (aperture, viewing angle, exposure time, illumination, type of quantization, coding, etc.) characterizing the multivariate states of the information-measuring system. Therefore, Table of the model $VM(K_i, X_i, Y_i)$ can be represented as a family of covariance matrices.

According to ISO/IEC Guide 98-3/Suppl 2:2011² the covariance matrix is a positively semidefinite matrix of dimension $N \times N$, where N is the number of input quantities, on the main diagonal of which there are squares of standard uncertainties corresponding to the estimates of the magnitude, and the remaining members of the matrix represent covariances between pairs of corresponding estimates of the elements of the magnitude:

$$u(x_{ji}, x_{kl}) = \frac{1}{m-1} \sum_{x \in C} (x_{ji} - \mu_1)(x_{kl} - \mu_2), \quad (4)$$

where μ_1, μ_2 are mathematical expectations by signs; C is multiple points in a class.

So for each j -th implementation, the dimension of the matrix will be 5×5 . To implement K_1 , the matrix has the form:

$$u_1(X_1 \dots X_5) = \begin{pmatrix} u^2(x_{11}) & u(x_{11}, x_{12}) & u(x_{11}, x_{13}) & u(x_{11}, x_{14}) & u(x_{11}, x_{15}) \\ u(x_{12}, x_{11}) & u^2(x_{12}) & u(x_{12}, x_{13}) & u(x_{12}, x_{14}) & u(x_{12}, x_{15}) \\ u(x_{13}, x_{11}) & u(x_{13}, x_{12}) & u^2(x_{13}) & u(x_{13}, x_{14}) & u(x_{13}, x_{15}) \\ u(x_{14}, x_{11}) & u(x_{14}, x_{12}) & u(x_{14}, x_{13}) & u^2(x_{14}) & u(x_{14}, x_{15}) \\ u(x_{15}, x_{11}) & u(x_{15}, x_{12}) & u(x_{15}, x_{13}) & u(x_{15}, x_{14}) & u^2(x_{15}) \end{pmatrix}. \quad (5)$$

The abbreviated form of writing this matrix:

$$u_{1ij} = \begin{cases} u^2(x_{1j}) & i = j \\ u(x_{1i}, x_{1j}) & i \neq j \end{cases}, \quad (6)$$

where $u^2(x_{ij})$ is variance of the estimate x_{ij} ; $u(x_{ij}, x_{mh})$ is covariance between values x_{ij} and x_{mh} .

Similarly, we write for implementations K_2 – K_5 . The uncertainty $u(Y_1)$ is calculated from the expression:

$$u(Y_i) = C u(X_i) C^T, \quad (7)$$

where C is matrix of sensitivity coefficients with dimension $N \times N$.

The sensitivity coefficients can be defined as partial derivatives of the original function f connecting the variables X_1, X_2, \dots, X_5 [15]:

$$C_j = \left(\frac{\partial f}{\partial x_j} \right). \quad (8)$$

For the case of the triad X_1, X_2, X_3 the covariance cube of the information and measurement system is shown in Figure 1 on the faces of which the matrix elements are located. There are only six triads as six faces of this cube can be displayed. In this case, the covariance cube contains $3 \times (m \times m)$ elements.

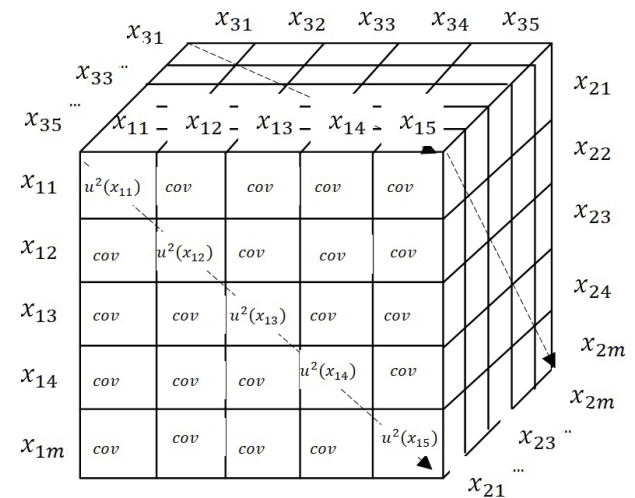


Figure 1 – Covariance cube of the information and measurement system $VM(K_i, X_1, X_2, X_3, Y_i), i = 1, \dots, m$

² ISO/IEC Guide 98-3/Suppl 2:2011 Uncertainty of measurement. Part 3: Guide to the expression of uncertainty in measurement (GUM:1995). Supplement 2: Extension to any number of output quantities

Considering that the covariance cube generally contains jWm^2 elements (where j is the number of variables X_j , and m is the number of implementations K_i), it can be further considered a covariance hypercube of the information and measurement channel.

Transition to orthogonal matrices of high dimensions

The problem of color multivariance in digital colorimetry is solved with the help of orthogonal matrices of high dimensions that allow displaying the states of the information and measurement channel in a multidimensional space. The graphical representation of a hypercube through 5-matrices with fixed (a, b, c) and sliding (α, β, γ) indices in the form of a set of 3-matrices of n -dimensions can be

represented compactly in the interpretation of Penrose diagrams [16, 17], as illustrated in Figure 2.

This diagram is an image of multilinear functions or tensors and represents several shapes connected by lines. Each element of the original matrix is multiplied by the corresponding element of the convolution matrix. By the derivative f_x of the image f we will understand:

$$f_x(i, j) = \frac{\partial f(x, y)}{\partial x} \Big|_{\substack{x=x_i \\ y=y_j}} = f_{i,j} - f_{i-1,j}. \quad (9)$$

Under the convolution matrix, we will understand the matrix of coefficients which is “multiplied” by the values of the pixel intensities of the image to obtain the desired result. An example of such matrices used to detect lines in [18] is shown in Figure 3.

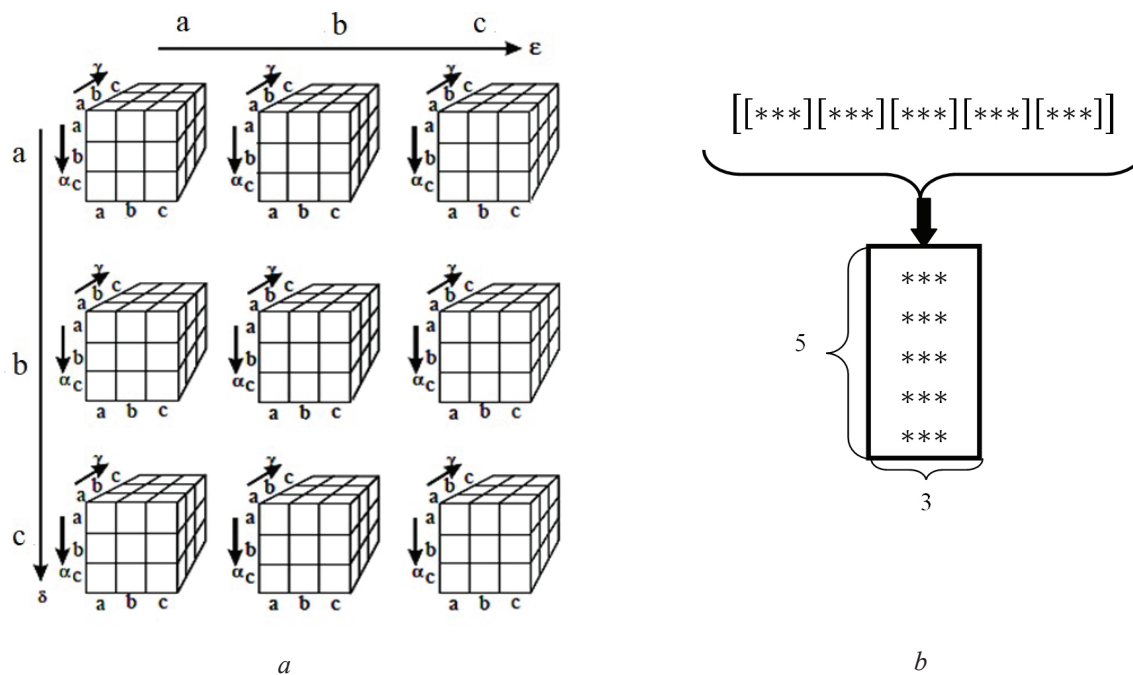


Figure 2 – Representation of the 5-matrix $A\alpha\beta\gamma\delta\epsilon$ in the form of a set of matrices: a – based on the Crohn’s methodology; b – in the form of Penrose diagrams

-1	-1	-1
2	2	2
-1	-1	-1

-1	-1	2
-1	2	-1
2	-1	-1

-1	2	-1
-1	2	-1
-1	2	-1

2	-1	-1
-1	2	-1
-1	-1	2

Figure 3 – Example of convolution matrices

Then the total sum of these products is found, which, if necessary, is divided by the normalization coefficient (the sum of the elements of the convolu-

tion matrix). This is necessary in order for the average intensity to remain unchanged. Then the brightness value of the current pixel can be set by the formula:

$$L_{ij} = \sum_{i=1}^{n \times m} w_i z_i, \quad (10)$$

where z_i is the brightness value of the pixel corresponding to the mask coefficient w_i .

For example a command in *Wolfram Mathematica* system, that displays the original image of the motherboard as well as its modified images, as shown in Figure 4 is written according to the developed program [19] as follows: `{f, ImageConvolve[f, maska1]//ColorNegate,`

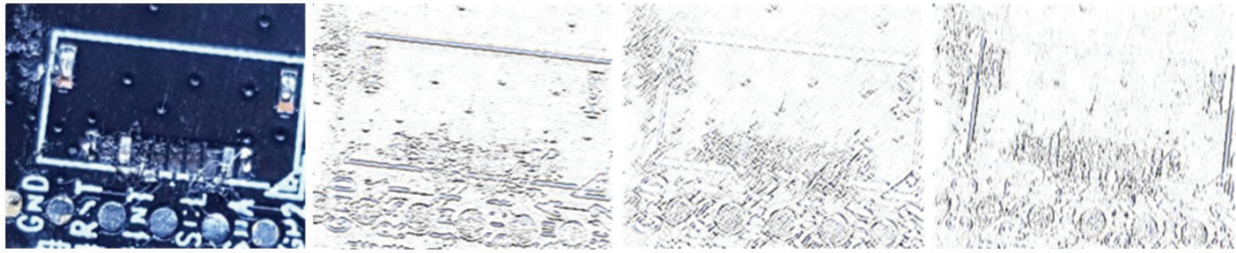


Figure 4 – Line detection on the motherboard snapshot

0.00987648	0.0796275	0.00987648
0.0896275	0.641984	0.0796275
0.00987648	0.0796275	0.00987648

Figure 5 – Convolution matrix

Matrix elements can be defined using the built-in function `GaussianMatrix` in the *Wolfram Mathematica* system.

Color tensors in spaces of directed fields

Taking into account the recording of orthonormalized matrices distributed according to the normal law for some image f the structural tensor takes the form (subscripts denote spatial derivatives and the dash indicates convolution with a Gaussian filter) [19]:

$$G = \begin{pmatrix} \overline{f_x^2} & \overline{f_x f_y} \\ \overline{f_x f_y} & \overline{f_y^2} \end{pmatrix}. \quad (11)$$

The tensor describes the local differentiated structure of the image and is suitable for finding edges and corners. The original image has the form:

$$f = \begin{pmatrix} R \\ G \\ B \end{pmatrix}. \quad (12)$$

`ImageConvolve[f, maska2]//ColorNegate, ImageConvolve[f, maska4]//ColorNegate}`.

The figure demonstrates the reduction of degrees of freedom due to the use of convolution matrices during the transition from full-color to half-tone and binary images. The most commonly used filter based on convolution matrices is the Gaussian filter (the matrix is filled according to the normal law). In this case, the elements of the matrix are normalized. An example of such a matrix is shown in Figure 5.

If the structural tensor G is considered a color tensor, then for the *RGB* color space it can be written as:

$$G = \begin{pmatrix} \overline{R_x^2 + G_x^2 + B_x^2} & \overline{R_x R_y + G_x G_y + B_x B_y} \\ \overline{R_x R_y + G_x G_y + B_x B_y} & \overline{R_y^2 + G_y^2 + B_y^2} \end{pmatrix}. \quad (13)$$

If a color tensor describes a two-dimensional structure at a certain point in the image then its own value can be determined for it by the formula [13, 20] (the superscript T denotes the transpose operation):

$$\lambda_1 = 0,5(\overline{f_x^T f_x} \overline{f_y^T f_y} + \sqrt{(\overline{f_x^T f_x} - \overline{f_y^T f_y})^2 + (2\overline{f_x^T f_y})^2}). \quad (14)$$

The parallel operation of determining the intensities of a digital image using a structural color tensor in the color channels R, G, B is carried out using the commands `ImageHistogram[f, Appearance->"Separated"]`, as shown in the Figure 6 [18].

The eigenvalue indicates the local orientation on the image with the maximum color change. The elements of the tensor G are invariant when the spatial axes rotate and move. This representation is applicable for classifying the color in the image taking into account situations when the color change is caused by a shadow or darkening of the image the influence of the presence of glare.

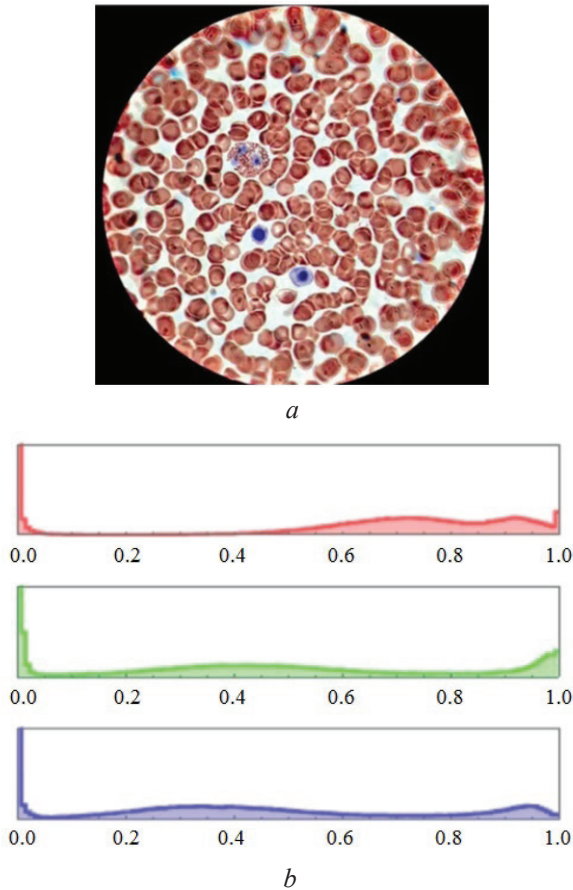


Figure 6 – The result of using a structural tensor: *a* – digital image of a blood sample obtained using a microscope; *b* – RGB-image histograms

The second-rank color tensor is described in [13] and is used to construct Macadam balls describing the *XYZ* color space as a “single-cavity hyperboloid in four-dimensional spacetime having the form” [13]:

$$R_{ab} - \frac{R}{2} g_{ab} = 0, \quad (15)$$

where R_{ab} is the Ricci curvature tensor obtained from the R_{abcd} space-time curvature tensor by convolving it by a pair of indices; R is scalar curvature that is, the collapsed Ricci tensor; g_{ab} is metric tensor.

Then you can map a certain color vector to any point on the color locus. “Since all vectors of type OS start from the zero point, the length of these vectors (color saturation) is determined by a simple expression of the type” [13]:

$$D = \sqrt{x^2 + y^2 + L^2}, \quad (16)$$

where x, y is coordinates of the end of the vector in the coordinate system $x^i y^j$; L is brightness of the end point of the vector.

The divalent symmetric color tensor G_{ab} can be expressed by decomposing the color vector g_i by the orthonormal basis e_1, e_2, e_3 [20]:

$$G_{ab} = \begin{pmatrix} H & 0 & 0 \\ 0 & S & 0 \\ 0 & 0 & L \end{pmatrix} = \begin{pmatrix} \arctg(x/y) & 0 & 0 \\ 0 & \sqrt{x^2 + y^2 + L^2} / \sqrt{x_a^2 + y_a^2 + L_a^2} & 0 \\ 0 & 0 & L \end{pmatrix}, \quad (17)$$

where H is color tone; S is saturation.

The essence of this tensor is to set the coordinates for the metric tensor at a specific point on the color diagram [13]. Moving from the single-cavity hyperboloid shown in Figure 7 to the standard color body of the *XYZ* space, we will deal with tensors of higher orders.

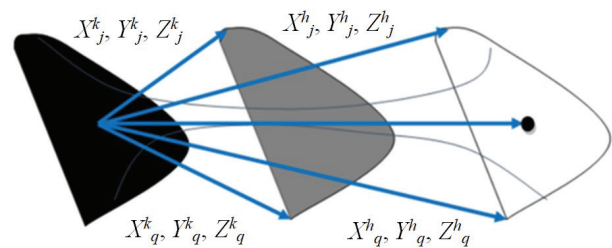
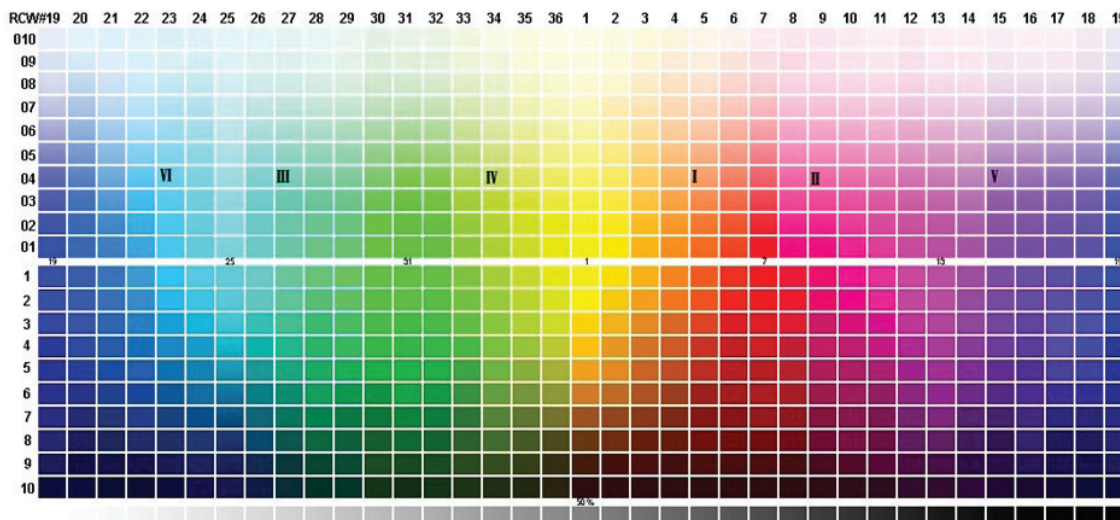


Figure 7 – Representation of the *XYZ* color space as a one-band hyperboloid with decomposition into families of vectors

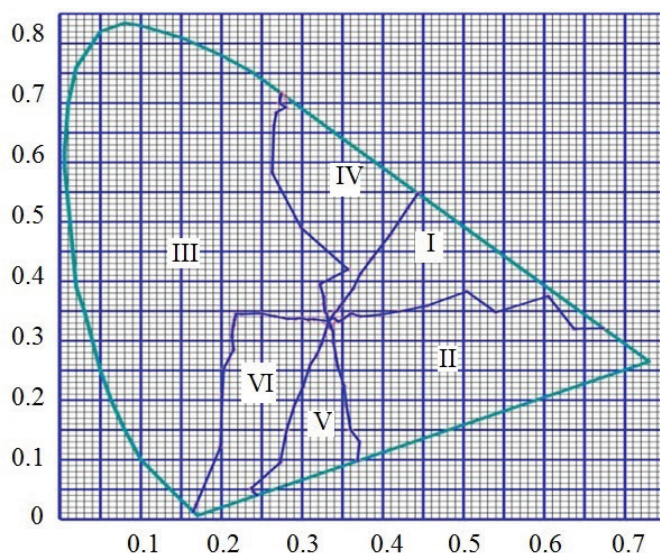
Tensors come out of the zero point, intersect the plane of the locus and can be combined into families of vectors $X^k_0 Y^k_0 Z^k_0, X^k_j Y^k_j Z^k_j, X^h_j Y^h_j Z^h_j, X^k_q Y^k_q Z^k_q, X^h_q Y^h_q Z^h_q$. They form directed fields by zoning the color body of the *XYZ* space [21] satisfying the expressions for calculating the chromaticity coordinates at the color locus [3]:

$$x = \frac{X}{X + Y + Z}; \quad y = \frac{Y}{X + Y + Z}; \quad z = \frac{Z}{X + Y + Z}. \quad (18)$$

The standardized palette (as an example, the palette shown in Figure 8a) is divided into six spatial sectors according to the principle of predominance of R (red), G (green) and B (blue) components (I – RGB ; II – RBG ; III – GBR ; IV – GRB ; V – BRG ; VI – BGR) and transformed into the coordinates of the *XYZ* space, whose chromaticity coordinates at the color locus represent the intersection points of the color tensors (Figure 8b) [21].



a



b

Figure 8 – Zoning of the XYZ color space: a – standardized computer palette; b – a color locus divided into sectors

Tensor indexing and singular value decomposition methodology [21] makes it possible to build low-rank approximations of matrices that require less space in computer memory and less computing resources to work with them.

Tensor calculus in discrete-quantized space

Multiple registration of a static object with incrementally increasing exposure time allows to determine the $R_j G_j B_j$ color coordinates for each implementation, combine them into vector families ($R_j^T G_j^T B_j^T$ tensor), transform them into $X_j Y_j Z_j$ vector families ($X_j^T Y_j^T Z_j^T$ tensor) moving from the

zero point to the plane of the color locus, expanding the dynamic range without losing metrological traceability. From the point of view of general relativity, such a displacement can be considered as a parallel transfer of some vector [23] A^i_0 from the starting point P_0 with coordinates $x^i_0 = x^i(\mu_0)$ along the curve $x^j = x^j(\mu)$ to the point P_1 with coordinates $x^i_1 = x^i(\mu_1)$, ($\mu_0 \leq \mu \leq \mu_1$) which connected to each other. The unique (according to Cauchy's theorem) vector $A^i_1 = A^i(\mu_1)$ is the result of parallel transfer and characterizes the value of the field $A^i(x(\mu))$ at the point of μ_1 . The vector gets incremented [22]:

$$\delta A^i = -\Gamma^i_{kj} \frac{dx^j}{d\mu} \delta x^j, \quad (19)$$

where δx^j is infinitesimal vector to which the transfer is carried out; Γ_{kj}^i is the coefficient of connectivity characterizing the degree of curvature of space.

The dynamics of open quantum systems in the language of tensor networks is described through Hamiltonians and the quantum reservoir model as a set of non-interacting quantum oscillators [22] whose dimension is greater than the dimension of the system. The quantum diagram of the dynamics of the system and the reservoir (upper and lower channels, respectively) [22] is shown in Figure 9.

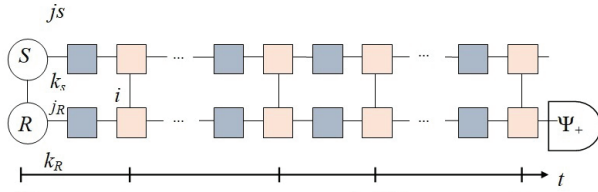


Figure 9 – Diagram representation of color space sampling in the form of a time tensor network

Connections i between two channels (system and reservoir) illustrate the correlation between reference points – physically implemented traceability sources j_s (standard samples) and their j_s images at certain points in time. The Hamiltonian of the complete system is generally given by the expression [22]:

$$H = H_0 + H_{\text{int}}, \quad (20)$$

where

$$H_0 = H_s \otimes I + I \otimes H_R; \quad (21)$$

$$H_{\text{int}} = \gamma \sum_{i=1}^n A_i \otimes B_i, \quad (22)$$

where H_s and H_R are hilbert spaces of the system and its reservoir, respectively; I is information; H_{int} is mutual information entropy between spaces; γ is characteristic constant of interaction between the reservoir and the system.

The dynamics of the complete system in the form of the Trotter expansion has the next form [22]:

$$|\rho(t)\rangle = \Phi_0(\tau)\Phi_{\text{int}}(\tau)\dots\Phi_0(\tau)\Phi_{\text{int}}(\tau)|\rho(t)\rangle + O(\gamma\tau), \quad (23)$$

where $\Phi_0(\tau)$ is dynamic mapping responsible for free dynamics over time τ ;

$$\Phi_0(\tau) = \exp(-i\tau H_s) \otimes \exp(i\tau H_s^T) \otimes \exp(-i\tau H_R) \otimes \exp(i\tau H_R^T), \quad (24)$$

$\Phi_{\text{int}}(\tau)$ is a dynamic map that is responsible for the dynamics only involving the interaction Hamiltonian over time τ . Parameter $O(\gamma\tau)$ specifies the accuracy

of the temporal tensor network with the sampling step τ . The time discreteness is given as $N = t/\tau$.

The process of color space quantization is conveniently viewed in terms of the depth of the reservoir's memory. Assuming that the initial state of the reservoir does not depend on the initial states of the system, we write an expression for the brightness levels B [22]:

$$\langle B_i(t + \delta t) B_j(t) \rangle = \frac{t}{\tau - 1} \dots i, \frac{\delta t}{\tau - 1} \dots j}{-\gamma\tau}. \quad (25)$$

The vector increment δt is the nominal quantization step. In terms of the memory depth T of the effective reservoir R , the mutual information between two quantum systems will be [22]:

$$I(L; R) = S(M_{L,R} \| M_L \otimes M_R) \sim \exp\left(-\frac{(p-q)\tau}{T}\right), \quad (26)$$

where M is arbitrary density reservoir temporary network matrix with a set of not necessarily orthogonal vectors $\{V_q\}_q$, represented in the form [22]:

$$M = \sum V_q V_q^+. \quad (27)$$

To select a sufficient dimension of the effective reservoir, the criteria of entanglement entropy, Rényi, and von Neumann are used in [22]. Renyi entropy is calculated by the formula $0 < \alpha < 1$ [22]:

$$S(M) = \frac{1}{1-\alpha} \ln \text{Tr} M^\alpha. \quad (28)$$

The relative entropy is zero if and only if. For the von Neumann entropy [22]:

$$d \approx \exp(2n\gamma T(1 - \ln \gamma\tau)). \quad (29)$$

Note that the contributions to the time evolution of the system from its previous states decrease exponentially as the time interval between the current and previous states of the system increases. The characteristic time interval in which the previous states of the system make a significant contribution is equal to the depth of the reservoir memory T , i. e. bits per channel [22].

Conclusion

Since digital colorimetry is based on the transformation of color spaces, their discretization, quantization, encoding and decoding, it is proposed to use the apparatus of tensor calculus to solve the problems of ensuring metrological traceability and reliability.

The presented validation model shows the multivariance of the states of the information-measuring channel through the phenomenon of the covariance hypercube. Only implementations with one unknown make it possible to perform measurements. The transition to orthogonal matrices of high dimensions leads to redundancy of information when identifying the states of the information-measuring system and its elements.

The proposed approach is based on the ranking of intensities in color channels and the division of color spaces into areas of directional fields, which makes it possible to reduce the uncertainty of color measurement. Parallel transfer of vectors with subsequent indexing of color tensors makes it possible to expand the dynamic range of digital image intensity.

A promising area of application of tensor calculus in digital colorimetry is the solution of inverse problems associated with the modeling of information and measurement systems, the creation of virtual objects, and exploratory studies of traceability under high uncertainty.

References

1. Fershil'd M.D. *Modeli cvetovogo vospriyatiya* [Color perception models]. Moscow, Tekhnosfera Publ., 2005, 416 p.
2. Kuznecov U.V. [Color Management Systems: Concept and Opportunity]. *Poligrafiya* [Polygraphy], 2005, no. 4, pp.14–17 (in Russian).
3. Schanda J. *Colorimetry: Understanding the CIE system*. New York, A John Wiley & SONS Publ., 2007, 467 p.
4. Fan Y., Li J., Guo Y., Xie L., Zhang G. Digital image colorimetry on smartphone for chemical analysis. *Measurement*, 2021, vol. 171, p. 108829.
DOI: 10.1016/j.measurement.2020.108829
5. Bure V.M., Mitrofanova O.A. Analysis of aerial photographs to predict the spatial distribution of ecological data. *Contemporary Engineering Sciences*, 2017, vol. 10, no. 4, pp. 157–163 (in Russian).
DOI: 10.12988/ces.2017.611175
6. Mitrofanov E.P., Petrushin A.F., Mitrofanova O.A. [Using aerial photography data to substantiate precision agricultural practices for the use of agrochemicals]. *Vtoraya vserossiyskaya nauchnaya konferenciya s mezhdunarodnym uchastiem "Primenenie sredstv distancionnogo zondirovaniya zemli v sel'skom hozyajstve"* [Second all-russian scientific conference with international participation "Application of earth remote sensing in agriculture"]. St. Petersburg, September 26–28, 2018, pp. 212–217 (in Russian).
7. Goden ZH. *Kolorimetriya pri videoobrabotke* [Colorimetry in video processing]. Moscow, Tekhnosfera Publ., 2008, 328 p.
8. *ICCExperts' Dayon HDR ColourImaging*. [Electronic Resource]. Available at: <https://www.color.org> (accessed: 15.03.2022).
9. *Parameter values for the HDTV standards for production and international programme exchange*. [Electronic Resource]. Available at: <https://www.itu.int/rec/R-REC-11> (accessed: 01.02.2022).
10. *Reference electro-optical transfer function for flat panel displays used in HDTV studio production*. [Electronic Resource]. Available at: <https://www.itu.int/rec/R-REC-BT.1886> (accessed: 01.02.2022).
11. *Image parameter values for high dynamic range television for use in production and international programme exchange*. [Electronic Resource]. Available at: <https://www.itu.int/rec/R-REC-BT.2100> (accessed: 01.02.2022).
12. *High dynamic range television for production and international programme exchange*. [Electronic Resource]. Available at: <https://www.itu.int/pub/R-REP-BT.2390> (accessed: 01.03.2022).
13. Lozhkin L.D., Voronov A.A., Soldatov A.A. Converting CIE color space to strictly equal contrast based on tensor calculus. *Fizika volnovykh processov i radiotekhnicheskie sistemy* [Physics of wave processes and radio engineering systems], 2016, vol. 19, no. 4, pp. 50–59 (in Russian).
14. Makarov D.G. Digital processing of television measuring signals. *Cifrovaya obrabotka signalov* [Digital signal processing], 2007, no. 3, pp. 30–36 (in Russian).
15. Saukova Y. The Validation Model of Information Measuring Channel in Technical Vision Systems. *International Journal of Advanced Engineering and Technology*, 2018, vol. 1, no. 4, pp. 28–33.
16. *Elementy tenzornogo analiza G. Krona* [Elements of tensor analysis G. Krohn]. [Electronic Resource]. Available at: <http://устойчивоеразвитие.рф/index.php?id=91> (accessed: 01.02.2022).
17. Luchnikov I., Vintskevich S., Ouerdane H., Filippov S. Simulation complexity of open quantum dynamics: Connection with tensor networks. *Physical Review Letters*, 2019, vol. 122, no. 16, p. 160401.
DOI: 10.1103/PhysRevLett.122.160401
18. Hundzina M.A. An overview of Wolfram Mathematica functions that implement image segmentation. *Mekhanika ta matematichni metodi* [Mechanics and mathematical methods]. Odessa, 2020, pp. 78–89.
19. Van de Weijer J., Robust J., Gevers T., Smeulders A.W.M. Photometric Invariant Features from the Color Tensor. *IEEE Transactions on Image Processing*,

2006, vol. 15, iss. 1, pp. 118–127.

DOI: 10.1109/TIP.2005.860343

20. Lozhkin L.D., Neganov V.A. *Cvet, ego izmerenie, vosproizvedenie i vospriyatie v televidenii. CHast' I* [Color, its measurement, reproduction and perception in television. Part I]. Samara, IUNL PGUTI Publ., 2013, 286 p.

21. Saukova Y., Matyush I. The Metrological Assurance of the Colorimetry in Software and Hardware En-

vironments. *International Journal of Innovative Research in Electronics and Communications (IJIREC)*, 2016, vol. 3, no. 5, pp. 6–19. **DOI:** 10.20431/2349-4050.0305002

22. Alekseev S.O., Pamyatnyh E.A., Ursulov A.V., Tret'yakova D.A., Rannu K.A. *Vvedenie v obshchuyu teoriyu otnositel'nosti, ee sovremennoe razvitie i prilozheniya* [Introduction to General Relativity, Its Modern Development and Applications]. Ekaterinburg: Izd-vo Ural. Un-t, 2015, 380 p.